7th International Conference on Creep, Fatigue and Creep-Fatigue Interaction (CF-7)
Indira Gandhi Centre for Atomic Research, Kalpakkam, Tamil Nadu, India. January 19-22, 2016
Invited Lecture

ALLOY BY DESIGN - A MATERIALS GENOME APPROACH TO ADVANCED HIGH STRENGTH STAINLESS STEELS FOR LOW AND HIGH TEMPERATURE APPLICATIONS

Qi Lu, Wei Xu and S. van der Zwaag*
Novel Aerospace Materials group, Faculty of Aerospace Engineering
Delft University of Technology, Kluyverweg 1, 2629 HS, Delft, The Netherlands
*Corresponding author e-mail: S.vanderZwaag@tudelft.nl

ABSTRACT

We report a computational 'alloy by design' approach which can significantly accelerate the design process and substantially reduce the development costs. This approach allows simultaneously optimization of alloy composition and heat treatment parameters based on the integration of thermodynamic, thermo-kinetics and a genetic algorithm optimization route. Novel steel compositions and associated key heat treatment parameters are identified so as to realize the target microstructure for applications either at the room temperature (ultra-high strength maraging stainless steel) or at high temperatures (creep resistant steels). Solid solution strengthening and precipitation hardening are the two strengthening mechanisms employed to improve the strength of designed steels. Either one of them or their combination is optimized in the four steel families considered. Each model is validated by analyzing the strengthening contributions in existing steels and by experimental characterization of prototype alloys. Very good agreement between experimental performance and model predictions is found. All newly designed alloys are predicted to outperform existing high end reference grades.

Keywords: Alloy design, Precipitation hardening, Solid solution strengthening, Matrix

1.0 INTRODUCTION

Advanced high strength stainless steels with improved strength and corrosion resistance are persistently demanded for the key components in high end applications in aerospace industry and power plants applications. These alloys generally have very complex compositions, alloyed with various elements for specific considerations, while avoiding particular species at the same time. Traditionally, such alloys were designed by the experimental trial and error approach starting from a reference alloy and hence this approach may (only) realize small stepwise improvements at best and at a low success rate [1-3]. Moreover, the design cycle may be extremely long and costly, especially for creep resistant steels, due to the complex interactions among alloying elements and necessarily long evaluation times.

From an alloy design viewpoint, the performance of a material is determined by both its 'genome' (inherent property, e.g. composition and element interactions) and its 'experience' (imposed processing and use -conditions) [4]. With the significant advances in understanding correlations between composition, processing, microstructure evolution and eventually the mechanical properties, the computational alloy design offers new possibilities to integrate considerations of 'genome' and 'experience' in the design phase, for example, artificial neural networks (ANN) [5, 6] and ab initio calculations [7-9]. ANN is a statistics rooted method which can take into account many parameters including both 'genome' and 'experience' types regardless their nature and the understanding of their roles. However, its prediction highly depends on the accuracy and number of data available. The ab initio calculation is a more physics funded approach from the atomic scale and hence intrinsically

inherits the 'genome' consideration, while it can also incorporate the 'experience' inputs to a limited extend in predicting the performance of a material. Nevertheless, ab initio calculations still require major simplifications and are not yet possible for complex stainless steel grades containing typically up to 9 alloying elements at widely different concentration levels.

The materials genome approach can be considered as encoded in the language of CALPHAD thermodynamics and kinetics [4], and it determines the microstructure evolution for a given 'experience'. Therefore, thermodynamics has been applied as a major guideline in discovering new alloys [10-13] wherein processing parameters were taken into account but in a non-integrated manner. In this study, we report a computational alloy design approach, which integrates the materials genome in form of thermodynamics/kinetics and the 'experience' parameters by considering the microstructure evolution and consequent effects on mechanical properties via physical metallurgy principles. The integrated alloy design approach allows to design and optimize the genome and experience parameters simultaneously. We first summarize our previous work, i.e. the design of advanced ultra-high strength stainless steels for room temperature use [14-19] and high temperature creep resistant stainless steels [20-23]. Then the approach is generalised to explore the composition-properties space for novel stainless creep resistant steels having different matrices (ferritic, martensitic or austenitic) strengthened by solid solution and being strengthened by different precipitates (MX carbonitrides or intermetallic Ni_3Ti). This part of work will be published elsewhere soon.

2.0 ALLOY BY DESIGN METHODOLOGY

The design methodology follows the philosophy of the 'goal/mean' orientation, from application to properties, to microstructures and eventually to the composition & processing conditions [24]. The performance of such a design process highly relies on two key steps as shown in Figure 1: the 'translator' for the correlation from mechanical properties to required microstructures, and the 'creator' to link desirable microstructures to alloy composition (genome) and heat treatments (experience) employing established metallurgical principles [25]. In the design of advanced stainless steels, the translator converts the required properties, such as high strength, good stability and decent oxidation or corrosion resistance, into desirable microstructures using known microstructure-property relationships. Subsequently, the creator links the tailored microstructural features to a specific composition and related heat treatment parameters/service conditions by establishing various criteria, by which the genome and experience are intergraded and evaluated upon thermodynamic and kinetic calculations coupled with associated processing/service conditions. The criteria are defined by the creator as indicated in Figure 1 and classified either as go/nogo or as optimization criteria reflecting different considerations/requirements. The go/nogo criteria are evaluated firstly to eliminate non-eligible solutions and then the optimization criteria are assessed to obtain an optimal performance factor. In order to avoid local optimization, no starting reference alloy is applied and a genetic algorithm is employed to search the entire combinations of variables and to achieve the optimal solution effectively and efficiently.

The actual optimization route follows the direction of the red arrows. The genetic algorithm generates random solutions (combinations of composition and heat treatment parameters), over wide ranges which were set considering the physical and practical constraints. Necessary calculations to evaluate the go/nogo criteria can therefore be performed accordingly and only for those fulfilling all go/nogo criteria, which suggests that desirable

microstructure is obtained, are eligible for further extra calculations to evaluate and optimize the performance factor as listed in Table 1. The definition of these performance/ optimization factors are described in the following passages.

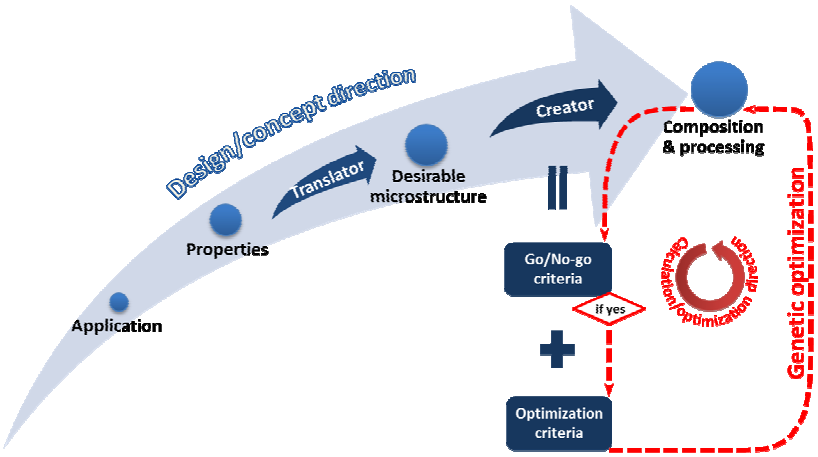

Figure 1 Flow chart of the alloy design strategy and optimization.

To obtain the microstructure strategy and strengthening mechanisms of chosen two examples, the translator has to consider the microstructure evolution and detail the corresponding requirements throughout the entire heat treatment, as summarized in Table 1. The creator therefore generates quantitative criteria associated to each microstructure requirement based on physical metallurgical principles. The quantities of creator as shown in Table 1 are calculated either by thermodynamics (via ThermoCalc®) at the corresponding temperatures or physical metallurgy formulas, e.g. all phase fractions/compositions are calculated by thermodynamics in an equilibrium state and T_{Ms} is martensite starting temperature which is calculated by an empirical formula as a function of austenite composition and used to ascertain the occurrence of the martensitic transformation upon cooling to room temperature.

Table 1. Key parameters in the Translator and creator for each type of target alloy:

	Translator: desirable microstructure			Creator: link the microstructure to composition and heat treatment				
				Go/nogo criteria				**Optimisation criteria/ Performance factor**
	Austenitization/ annealing temperature	Room temperature	Ageing/Service temperature	Austenitization/annealing temperature		T_{Ms} (K)	Ageing/Service temperature	
MAS	Austenite	Martensite	Martensite with sufficient Cr + maximal precipitates (MC carbide\Cu\Ni3Ti)	$V_{Austenite}$ > 99 vol.%	No liquid $V_{primary\ carbide}$ < 0.5 vol.%	>473	Cr in matrix> 12 mass % Undesirable phase< 1 vol.%	$\Delta\sigma_p$
FCS	Ferrite	Ferrite	Ferrite with sufficient Cr and best solid solution in matrix	$V_{Ferrite}$ > 99 vol.%		None		$\Delta\sigma_{ss}$
ACS	Austenite	Austenite	Austenite with sufficient Cr + optimal precipitates (MX carbonitride)	$V_{Austenite}$ > 99 vol.%		<298	Cr in matrix>16 mass% Sigma< 4 %vol.%, Undesirable phase (Sigma phase excluded)<1vol.%	$\Delta\sigma_{p(t)}$
MCS	Austenite	Martensite	Martensite with sufficient Cr + best solid solution + optimal precipitates (MX carbonitride)			>473	Cr in matrix>11 mass% Undesirable phase<1 vol.%	$\Delta\sigma_{p(t)}$ & $\Delta\sigma_{ss}$

The details of performance factors for different alloys as listed in Table 1 is introduced in the following. The PH contribution depends on the precipitate volume fraction, particle size and distribution. The MAS is designed to use at room temperature and therefore the precipitation contribution is determined by the ageing treatment and remains stable during it application. the precipitation contribution upon finishing of the ageing treatment can be estimated as:

$$\Delta\sigma_p = \alpha f_p^{1/2} r_0^{-1/2} \tag{1}$$

where $\Delta\sigma_p$ is the strengthening contribution due to precipitation, α is a constant, f_v is the equilibrium volume fraction of the precipitate. r_0 is the critical radius given by,

$$r_0 = 2\gamma / \Delta G \tag{2}$$

where γ is the interfacial energy, and ΔG is the driving force of precipitation at the ageing temperature. Different solutions can be found depending on the type of desired precipitate (Carbide MASCAR, Cu rich precipitates MASCU, or Ni_3Ti precipitates MASNITI)

Unlike the case of MAS, the PH in creep resistant steels varies with time and temperature due to significant growth and coarsening of precipitates during the service. Considering the coarsening kinetics [26-28], the PH contribution $\sigma_{p(t)}$ is estimated as

$$\Delta\sigma_{p(t)} \propto 1/L = \sqrt{f_p}/r = \sqrt{f_p}/\sqrt[3]{r_0^3 + Kt} \tag{3}$$

in which

$$K = 8\gamma V_m^{\,p} / \sum_{i=1}^{n} \frac{9(x_i^p - x_i^{mp})^2}{x_i^{mp} D_i / RT} \tag{4}$$

where L is the average inter-particle spacing, K is the coarsening rate, t is the exposure time at the high temperature, x is the equilibrium interfacial concentrations (in mole fraction) of the relevant chemical element on both the matrix (m) and the precipitate (p) sides, V_m^p is the molar volume of precipitate, T is the service temperature and D is corresponding diffusion coefficient. The necessary thermodynamic values including x_i^p, x_i^{mp}, D_i and V_m^p are obtained via Thermo-Calc® using the TCFE6 and Mob2 databases. For lack of information on the actual change in surface tension with chemical composition, this value is kept constant and set to a value of 1 $J/m^{2.}$.

Despite of the evolution of PH strengthening during the service, composition of the matrix remains a constant once the thermodynamic equilibrium is achieved and hence the SSS in the matrix also remain stable. Therefore , the SSS is defined as [29, 30],

$$\Delta\sigma_{ss} = a_1 \sum_i K_i C_i \tag{5}$$

Where $\Delta\sigma_{ss}$ is solid solution strengthening contribution, a_1 is a temperature dependent scale factor, K_i and C_i are the strengthening coefficient and atomic fraction of element i in the matrix. The values of K_i for different elements, such as Mo, W and Ni, in ferritic and austenitic matrices can be found in [28, 31, 32].

3.0 RESULTS AND DISCUSSION

The two examples chosen are the design of ultra-high strength maraging stainless steel (MAS) for room temperature application and the design of advanced creep resistant steels for high temperature use, taking into account the three matrix types possible (Ferritic (FCS), Martensitic (MCS), Austenitic (ACS). Each matrix may effectively employ different (combinations of) specific strengthening mechanisms, i.e., FCS utilizes solid solution strengthening (SSS); MAS and ACS apply precipitation hardening (PH) while MCS

combines both SSS and PH mechanisms. In the steel grades to be optimised the grain size, a non-thermodynamically addressable quantity, only plays a minor role in achieving the required performance level. Values of SSS and PH are calculated combining thermodynamics and metallurgical formula. Details of SSS and PH calculation are given in the "alloy by design methodology" section.

In order to validate the PH and SSS formulas employed, the calculated PH and SSS values of various existing ferritic, martensitic and austenitic creep resistant steels on the basis of alloy composition and use time are compared to experimental values. The results are shown in Figure 2. Notwithstanding the different matrix types and in strengthening mechanisms, a very good agreement between the calculated strength and existing experimental results can be obtained, which indicates that computational evaluations of the strengthening contributions of various types are appropriate and can be implemented in discovering new alloys.

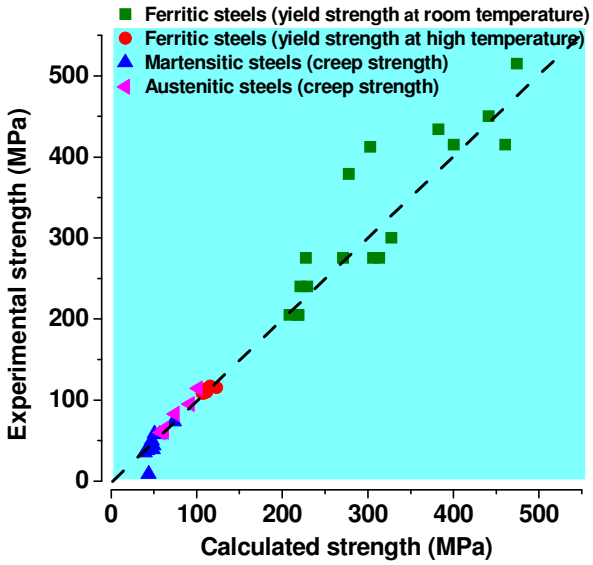

Figure 2. Calculated strength vs. experimental strength for the four different types of stainless steels considered

Applying the approach, the optimal compositions and heat treatment parameters of MAS, FCS, MCS and ACS steels are optimised. To demonstrate potentials of newly designed alloys, they are benchmarked to the existing high-end counterparts. Figure 3a shows the comparison of designed MAS and existing ultra-high strength stainless steels. The MAS alloys designed to be strengthened by MX carbides, Copper particles or Ni_3Ti intermetallic are labelled as MASCAR, MASCU and MASNITI respectively. Existing steel grades are seen to be described very well without any additional fitting, but more importantly all three newly designed MAS alloys are predicted to substantially outperform existing commercial grades. Furthermore, high resolution TEM analysis of prototype alloys has verified the presence of precipitates of the exact targeted type, i.e. carbide precipitates, copper particles and Ni_3Ti intermetallics, as shown in the figure. These results verify the robustness of thermodynamic database and potentials of the alloy design approach presented.

Figure 3b shows the separate contributions of solid solution and precipitation strengthening in both newly designed creep resistant steels FCS, MCS, ACS and their existing commercial counter-partners. Alloy FCS, which is designed to be strengthened by SSS only has a significantly higher SSS than existing ferritic creep resistant steels. Similarly, Alloy ACS,

which is optimized solely for PH, suggests a much higher PH than those of existing austenitic ones. Finally the MCS, which optimally combines the PH and SSS, indicates a Pareto front consisting of new solutions substantially superior to existing counterparts both in SSS and PH contributions. To construct this Pareto front, two separated optimisations were performed respectively: either only for PH factor, or only for SSS factor, and then put all the qualified solutions together. The turning point in the Pareto front indicates the best composition (alloy MCS) indicated by the arrow. Moreover, other composition on the Pareto front can also have better PH and SSS than that of existing steels. Therefore, the current model can design alloy with exceptional SSS or PH, or combinations thereof.

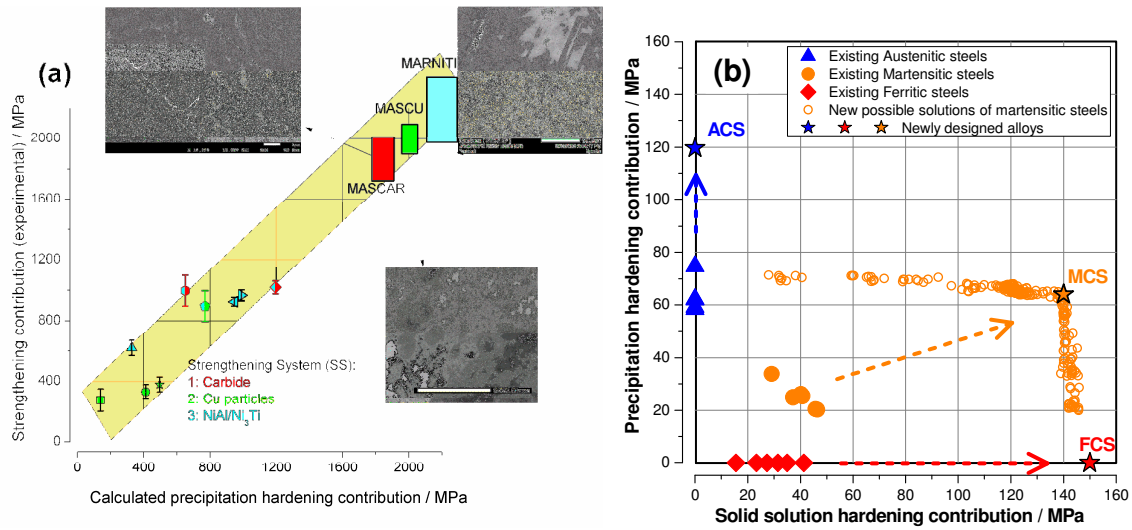

Figure 3. a) Comparison of existing and designed MAS steels. The precipitates in prototype of designed steels are identified by high resolution electron microscopy. The colour of symbols indicates the strengthening system and multiple precipitates/colours may occur in one alloy. b) Comparison of designed and existing creep resistant alloys.

The above study of simultaneous optimization of PH and SSS was applied to creep steels having a (tempered) martensitic matrix. We can extend the approach to other systems, for instance, simultaneous optimizing PH and SSS in austenitic or ferritic matrices. Moreover, MX carbonitride is not the only choice for the precipitate family, intermetallic can also applied as the desirable phase, such as Ni_3Ti. The results for austenitic, ferritic and martensitic matrices are presented in Figure 4a and 4b. Significant differences among three matrices can be found. Austenitic matrix can offer the highest PH contribution of MX carbonitrides, but the lowest SSS. Ferritic steel have the greatest capacity for SSS, have a PH contribution. While martensitic steels allow the best combination of both strengthening sources. These observations also apply to the Ni_3Ti system, albeit to a lesser degree as Ni_3Ti particles are harder to create at high volume fractions. In summary, the plots of Figure 4 clearly indicate the design space for a given matrix.

Precipitate coarsening (i.e. the 'experience' part in the optimisation) has a significant effect on the PH contribution in particular when the intended service time becomes 10^5 h or even longer. To demonstrate the effect of coarsening rates on the strength, the solutions in Figure 4b are taken as examples and each solution (dot) is mapped with its own coarsening rate, as shown in Figure 4c. Clearly, Ni_3Ti has the lowest coarsening rate in an austenitic matrix, followed by that in martensitic and ferritic matrices, respectively. This is due to the low diffusion rate of alloying elements in austenitic matrix. A lower coarsening rate also leads to a higher PH factor at the end of the service time. In addition, the solutions of NbX

carbonitride strengthened Martensitic steels on the Pareto front are also chosen and mapped with coarsening rates, as indicated in Figure 4c. The coarsening rates of NbX carbonitride are much slower than those of Ni_3Ti in martensitic matrix, indicating that carbonitrides are the preferred precipitate family for applications with ultra-long service time.

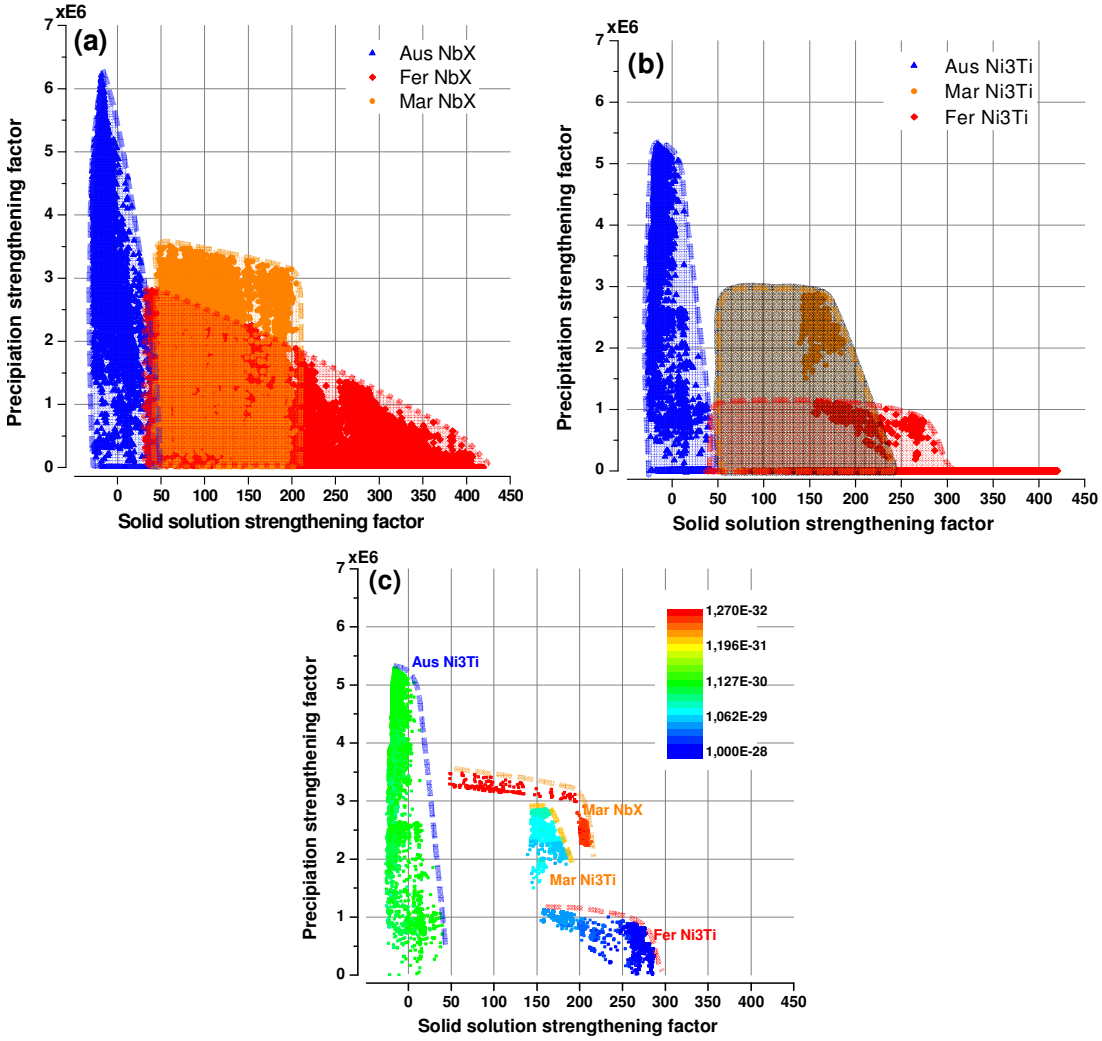

Figure 4. a) optimisation of PH of NbX cabonitride and SSS in austenitic, martensitic and ferritic matrices, b) optimisation of PH of Ni_3Ti and SSS in austenitic, martensitic and ferritic matrices, c) mapping the solutions in Ni_3Ti strengthened systems with coarsening rates. In addition, the solutions on Pareto front of NbX carbonitride strengthened Martensitic steels are also mapped with coarsening rate and shown in c) to compare to Ni_3Ti with the same matrix.

4.0 CONCLUSIONS

The genome approach works well for stainless steels and yields precisely defined composition and heat treatment ideally suited to start experimental development programs aimed at validation of the predicted high performance levels and addressing all pertinent technological challenges. The predicted optima are unlikely to be found in a realistic time via an empirical approach and the results as presented here clearly demonstrate that the Materials Genome approach holds great promise of substantially shortening the development time of new high performance steel grades.

ACKNOWLEDGEMENTS

This work was carried out with financial support from the Chinese Scholarship Council (CSC) and internal funding of TU Delft.

REFERENCES

1. M. Taneike, F. Abe, K. Sawada, Nature, **424** (2003) 294
2. K. Sawada, M. Taneike, K. Kimura, F. Abe, ISIJ Int., **44** (2004) 1243.
3. T. Horiuchi, M. Igarashi, F. Abe, ISIJ Int., **42** (2002) S67.
4. L. Kaufman, J. Ågren, Scr. Mater., **70** (2014) 3.
5. H.K.D.H. Bhadeshia, ISIJ Int., **41** (2001) 626.
6. S. Mandal, P.V. Sivaprasad, S. Venugopal, K.P.N. Murthy, B. Raj, Mater. Sci. Eng., A, **485** (2008) 571.
7. L. Vitos, P.A. Korzhavyi, B. Johansson, Nat. Mater., **2** (2003) 25.
8. G.P.M. Leyson, L.G. Hector Jr, W.A. Curtin, Acta Mater., **60** (2012) 387.
9. D. Raabe, B. Sander, M. Friák, D. Ma, J. Neugebauer, Acta Mater., **55** (2007) 4475.
10. P. Michaud, D. Delagnes, P. Lamesle, M.H. Mathon, C. Levaillant, Acta Mater., **55** (2007) 4877.
11. Z.K. Teng, F. Zhang, M.K. Miller, C.T. Liu, S. Huang, Y.T. Chou, R.H. Tien, Y.A. Chang, P.K. Liaw, Intermetallics, **29** (2012) 110.
12. V. Knežević, J. Balun, G. Sauthoff, G. Inden, A. Schneider, Mater. Sci. Eng., A, **477** (2008) 334.
13. C.E. Campbell, G.B. Olson, J. Comput. Aided Mater. Des., **7** (2000) 145.
14. W. Xu, P.E.J. Rivera-Díaz-del-Castillo, W. Yan, K. Yang, D. San Martín, L.A.I. Kestens, S. van der Zwaag, Acta Mater., **58** (2010) 4067.
15. W. Xu, P.E.J. Rivera-Díaz-del-Castillo, W. Wang, K. Yang, V. Bliznuk, L.A.I. Kestens, S. van der Zwaag, Acta Mater., **58** (2010) 3582.
16. W. Xu, P.E.J. Rivera-Díaz-Del-Castillo, S. van der Zwaag, Comput. Mater. Sci., **45** (2009) 467.
17. W. Xu, P.E.J. Rivera-Díaz-Del-Castillo, S. van der Zwaag, Philos. Mag., **88** (2008) 1825.
18. W. Xu, P.E.J. Rivera-Díaz-Del-Castillo, S. van der Zwaag, Philos. Mag., **89** (2009) 1647.
19. W. Xu, P.E.J. Rivera-Díaz-del-Castillo, S. van der Zwaag, Comput. Mater. Sci., **44** (2008) 678.
20. Q. Lu, W. Xu, S. van der Zwaag, Philos. Mag., **93** (2013) 3391.
21. Q. Lu, W. Xu, S. van der Zwaag, Comput. Mater. Sci., **84** (2014) 198.
22. Q. Lu, W. Xu, S. van der Zwaag, Acta Mater., **64** (2014) 133.
23. Q. Lu, W. Xu, S. van der Zwaag, Acta Mater., **77** (2014) 310.
24. G.B. Olson, Science, **277** (1997) 1237.
25. W. Xu, Q. Lu, X. Xu, S. van der Zwaag, Comput. Methods in Mater. Sci., 13 (2013) 382.
26. A. Kelly, Philos. Mag., **3** (1958) 1472.
27. J. Ågren, M.T. Clavaguera-Mora, J. Golczewski, G. Inden, H. Kumar, C. Sigli, Calphad-Computer Coupling of Phase Diagrams and Thermochemistry, **24** (2000) 41.
28. W.C. Robert, P. Haasen, Physical Metallurgy, Elsevier, Amsterdam, North-Holland, 1996.
29. H. Suzuki, Dislocations and mechanical properties of crystals, John Wiley, New York, 1957.
30. H. Zhang, B. Johansson, R. Ahuja, L. Vitos, Comput. Mater. Sci., **55** (2012) 269.
31. F.B. Pickering, Physical metallurgy and the design of steels, Applied Science Publishers LTD, London, 1978.
32. J.S. Wang, M.D. Mulholland, G.B. Olson, D.N. Seidman, Acta Mater., **61** (2013) 4939.